Calculation of the η and η' masses in the bag model

John F. Donoghue and Harald Gomm
Department of Physics and Astronomy, University of Massachusetts, Amherst, Massachusetts 01003
(Received 17 June 1983)

The annihilation contribution to the masses of the $J^{PC}=0^{-+}$ isoscalars is calculated in the bag model. The resultant mass shift for the η' is large and positive. For $\alpha_s=1.15$ we obtain $m_\eta=0.53$ GeV and $m_{\eta'}=0.965$ GeV, leading to a good description of pseudoscalar masses within the model.

I. INTRODUCTION

A decent understanding of the masses of the ground-state mesons and baryons has emerged from the quark model when one incorporates certain features of quantum chromodynamics.[1,2] In the MIT bag model even the light mass of the pion, and its expansion about the chiral limit, can be accounted for.[13] However, two states whose masses are not understood in the quark model are the η and η'. It is the purpose of this paper to calculate the lowest-order diagrams which are needed to explain these masses. We will show that this calculation has several interesting features, and that the result gives a reasonable description of the mass spectrum and of η-η' mixing.

It was long thought that both the η and the η' should be Goldstone bosons in the chiral limit (i.e., all quark masses being zero). Expansion about this limit then produces η and η' masses which are much too light.[4] This was known as the U(1) problem, and is seen in the quark-model context by the models predicting an isoscalar state degenerate with the pion when all diagrams to $O(\alpha_s)$ are included. The general resolution to this problem has come through a better understanding of the axial-vector anomaly.[5] In the chiral limit only an octet of Goldstone bosons exists, with the singlet ($\approx\eta'$) being massive. It is only in the dual limit of all quarks being massless and the number of colors tending to infinity (with g^2N_c fixed) that the η' becomes massless.[6] In quark models, these features are thought to be contained in the diagram of Fig. 1, plus similar but higher-order processes with more gluons.[1,7] This diagram shifts only the mass of the SU(3) singlet [if SU(3) breaking is small], and can make the singlet heavy, and also vanishes in the large-N_c limit.

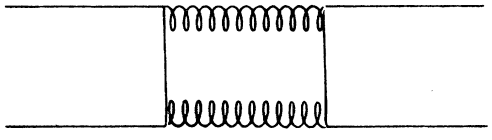

FIG. 1. The annihilation diagram which is responsible for the large mass of the η'.

This diagram, which we will refer to as the annihilation process, is clearly of order α_s^2. However, to explore the effect of it, it is not necessary to compute all $O(\alpha_s^2)$ corrections. Rather, the annihilation diagram, which occurs only in the isosinglet channel, can be separated from all others by comparison with nonisosinglet states such as the π and K. What one calculates is then a shift of the η' mass *relative* to the pion and kaon masses. This procedure is gauge invariant.

There is one feature which, on the surface, appears puzzling about the use of Fig. 1 to generate a large η' mass. If one looks at the intermediate state, it appears as if this diagram represents the mixing of a $q\bar{q}$ state with a two-gluon glueball. However, we know from second-order perturbation theory that such mixing always *lowers* the mass of the ground state. This would push the η' mass down instead of up. It is of general interest then to see what mechanism leads to positive sign for the mass shift. We will see that the dominant effect is *not* mixing with a glueball. In Coulomb gauge, which we will adopt in this paper, it arises from the replacement of one of the gluons with the instantaneous Coulomb interaction. In a covariant gauge, such a result would correspond to one of the gluons being an (unphysical) timelike component, which has an opposite sign, due to the metric, in its coupling.

This subject has also been considered in the bag context by Maciel and Monaghan.[8] Their conclusion on the sign of the amplitude is the same as ours, but we strongly disagree with the magnitude. Note that these authors also disagree with the magnitude of two published calculations on η'-glueball mixing.

The plan of the paper is as follows. In the next section we set up the general outline of the calculation. In Sec. III, one of the diagrams is presented in detail in order to display our methods. The results are given in Sec. IV and we calculate the mass spectrum and η-η' mixing with encouraging results. Finally Sec. V presents a brief summary.

II. THE METHOD OF CALCULATION

As mentioned in the Introduction, we will use the Coulomb gauge. To the order which we need it, the Coulomb-gauge Hamiltonian is given by

$$H=\int d^3x\,\bar{\psi}\left[i\vec{\gamma}\cdot\vec{\nabla}-g\vec{\gamma}\cdot\vec{A}^a\frac{\lambda^a}{2}+m\right]\psi$$
$$+\tfrac{1}{2}\int d^3x\,d^3y\,\psi^\dagger(x)\frac{\lambda^a}{2}\psi(x)G(\vec{x},\vec{y})\psi^\dagger(y)\frac{\lambda^a}{2}\psi(y)$$
$$+\cdots\,. \tag{1}$$

As pointed out by Friedberg and Lee,[9] the Green's function $G(x,y)$ is modified from its free-field value $(1/4\pi\,|\,\vec{x}-\vec{y}\,|\,)$ by boundary terms required by confinement

$$G(x,y)=\sum_{l,m}\frac{1}{2l+1}Y_{lm}(\hat{x})Y^*_{lm}(\hat{y})\left[\frac{r_<{}^l}{r_>{}^{l+1}}-\frac{x^l y^l}{R^{2l+1}}\right]. \tag{2}$$

Higher-order terms, and interactions involving only gluons, do not enter our calculations and are not displayed. There are then two types of interactions in this gauge. One involves the interaction of quarks with physical transverse gluons at order g, denoted as in Fig. 2(a). The other is the instantaneous Coulomb interaction at order g^2, as in Fig. 2(b). This is a conceptual advantage of Coulomb gauge as it explicitly separates out the physical gluonic degrees of freedom, the transverse gluons, from other gluonic effects such as the Coulomb potential.

We will also use old-fashioned time-ordered perturbation theory, with the propagators being expressed as a sum over bag-model eigenmodes. This leads to considerable algebraic complexity for the resulting expressions; however, we do not know of any easier method for the present calculation. Note that the annihilation diagram is finite, so that we need not worry about separating out divergent contributions, such as has proved troublesome in the mode-sum method.

To describe the effect of the annihilation diagram, we form the effective Hamiltonian for $q\bar{q}\to q'\bar{q}'$ by a consideration of the S matrix:

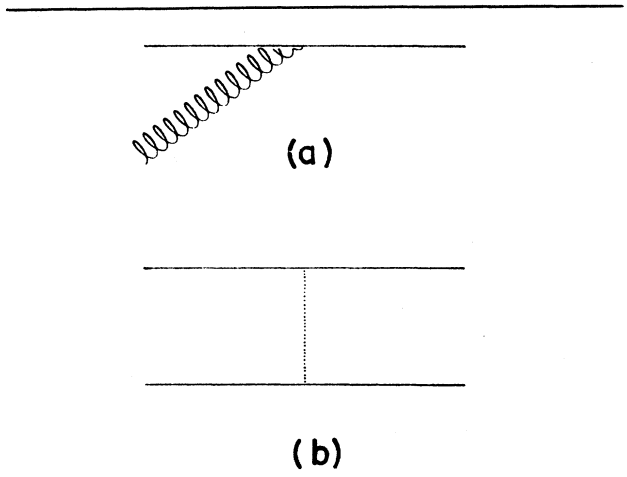

FIG. 2. (a) The coupling of a transverse gluon to quarks. (b) The instantaneous Coulomb interaction.

$$S_{fi}=\langle 0^{-+}\,|\,U(\infty,-\infty)\,|\,0^{-+}\rangle$$
$$=\left\langle 0^{-+}\left|T\exp\left[-i\int_{-\infty}^{\infty}H_I dt\right]\right|0^{-+}\right\rangle. \tag{3}$$

The interaction Hamiltonian contains transverse and Coulombic terms

$$H_I(x)=H^T(x)+H^C(x)\,, \tag{4}$$

which can be read off from Eq. (1). The perturbative expansion of the S matrix leads to the diagrams of Fig. 3. In particular Fig. 3(a) is obtained from

$$\tfrac{1}{24}\int d^4x\,d^4y\,d^4z\,d^4r\,T(H^T(x)H^T(y)H^T(z)H^T(r))\,, \tag{5}$$

while

$$\frac{i}{2}\int d^4x\,d^4y\,d^4z\,T(H^T(x)H^T(y)H^C(z)) \tag{6}$$

generates Fig. 3(b). A diagram with two factors of $H^C(x)$ would only contribute to positive-parity states. An effective Hamiltonian can be defined by

$$S_{fi}=-2\pi i\delta(E_i-E_f)\langle 0^{-+}\,|\,H_{\rm eff}\,|\,0^{-+}\rangle\,. \tag{7}$$

Expansion of $\langle 0^{-+}\,|\,H_{\rm eff}\,|\,0^{-+}\rangle$ reproduces term by term the corrections to the energy in time-independent perturbation theory.

III. CALCULATION

To illustrate the necessary computations we will explicitly calculate one of the time-ordered diagrams as given in Fig. 3(a). We will first give the solutions for the quark and gluon eigenmodes needed for the internal propagators, and then proceed to evaluate the diagram.

Solving the Dirac equation of motion in the bag leads to the quark wave functions

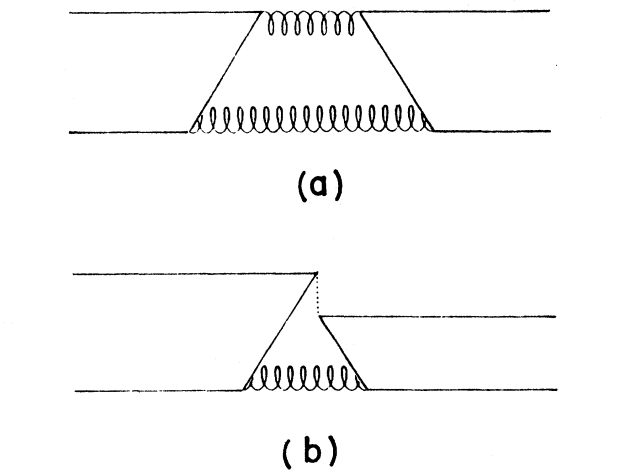

FIG. 3. The types of contributions which emerge from Fig. 1 when studied in the Coulomb gauge. There are many time orderings implied by each of these diagrams. These are found by permuting the vertices in all possible ways.

$$q_{l+1/2,m}(\vec{x})=N_{l+1/2}\begin{bmatrix}\alpha j_l(x_l r)\\ i\alpha'\vec{\sigma}\cdot\hat{r}j_{l+1}(x_l r)\end{bmatrix}\chi_{l+1/2,m}e^{-i\omega_l t},$$

$$q^c_{l+1/2,m}(\vec{x})=N_{l+1/2}\begin{bmatrix}\alpha'\vec{\sigma}\cdot\hat{r}j_{l+1}(x_l r)\\ i\alpha j_l(x_l r)\end{bmatrix}i(-1)^{m-1/2}\chi_{l+1/2,-m}e^{+i\omega_l t},$$

$$q_{l-1/2,m}(\vec{x})=N_{l-1/2}\begin{bmatrix}\alpha j_l(x_l r)\\ -i\alpha'\vec{\sigma}\cdot\hat{r}j_{l-1}(x_l r)\end{bmatrix}\chi_{l-1/2,m}e^{-i\omega_l t},$$

$$q^c_{l-1/2,m}(\vec{x})=N_{l-1/2}\begin{bmatrix}\alpha'\vec{\sigma}\cdot\hat{r}j_{l-1}(x_l r)\\ -i\alpha j_l(x_l r)\end{bmatrix}i(-1)^{m+1/2}\chi_{l-1/2,-m}e^{i\omega_l t},$$

$$\alpha=\left[\frac{\omega+m}{\omega}\right]^{1/2},\quad \alpha'=\left[\frac{\omega-m}{\omega}\right]^{1/2},\quad \omega_l{}^2=x_l{}^2+m^2, \tag{8}$$

$$\chi_{l+1/2,m}=\frac{1}{(2l+1)^{1/2}}\begin{bmatrix}(l+\frac{1}{2}+m)^{1/2}Y_{l,m-1/2}\\ (l+\frac{1}{2}-m)^{1/2}Y_{l,m+1/2}\end{bmatrix},$$

$$\chi_{(l+1)-1/2,m}=\vec{\sigma}\cdot\hat{r}\chi_{l+1/2,m},$$

$$N_{l\pm1/2}{}^{-2}=\int[\alpha^2 j_l{}^2(x_l r)+\alpha'{}^2 j_{l\pm1}{}^2(x_l r)]r^2dr.$$

Quark and antiquark wave functions are related by charge conjugation

$$q_c=i\gamma_2 q^*,$$

and the eigenvalues for $l\pm\frac{1}{2}$ quarks are fixed by the solutions of

$$\alpha j_l(x)=\pm\alpha' j_{l\pm1}(x). \tag{9}$$

For gluons there are two families of wave functions in the free-field limit:

$$\vec{A}^{\rm TE}_{lm}=\frac{1}{[2l(l+1)]^{1/2}}N_l j_l(\omega_l r)\vec{\mathscr{L}}Y_{lm}e^{-i\omega t}a^a_{lm}+\text{H.c.},\quad N_l{}^{-2}=\omega_l\int j_l{}^2r^2dr,$$

$$\vec{A}^{\rm TM}_{lm}=\frac{N_l}{[2l(l+1)]^{1/2}}\left[\frac{(l+1)j_{l-1}-lj_{l+1}}{2l+1}\hat{r}\times\vec{\mathscr{L}}Y_{lm}+i\frac{l(l+1)}{2l+1}(j_{l-1}+j_{l+1})\hat{r}Y_{lm}\right]a^a_{lm}+\text{H.c.}, \tag{11}$$

$$N_l{}^{-2}=\frac{\omega_l}{2l+1}\int[(l+1)j_{l-1}{}^2+lj_{l+1}{}^2]r^2dr.$$

The eigenvalues are given by

$$xj_{l-1}(x)-lj_l(x)\ \text{ for TE gluons},\quad j_l(x)=0\ \text{ for TM gluons}. \tag{12}$$

In evaluating the diagram, we use the notation $q_{0+1/2,s}\equiv q_s$ and $q_{k+1/2,l}\equiv q_k$, and obtain (sums over magnetic quantum numbers are implied)

$$\langle 0^{-+}\,|\,H_{\rm eff}\,|\,0^{-+}\rangle\to i\frac{g^4}{6}\int_{-\infty}^{x_0}dy_0\int_{-\infty}^{y_0}dz_0\int_{-\infty}^{z_0}dr_0(\bar{q}_s\mathcal{A}^{a\,\rm TE}_{m,n}q_k)(x)(\bar{q}_k\mathcal{A}^{b\,\rm TM}_{m,-n}q^c_{-s})(y)(\bar{q}^C_{s'}\mathcal{A}^{*a\,\rm TE}_{m,n}q_{k'})(z)(\bar{q}_{k'}\mathcal{A}^{*b\,\rm TM}_{m,-n}q_{-s'})(r)$$

$$\times\,\mathrm{tr}\frac{\lambda^a}{2}\frac{\lambda^b}{2}\mathrm{tr}\frac{\lambda^a}{2}\frac{\lambda^b}{2}d^3x\,d^3y\,d^3z\,d^3r. \tag{13}$$

The time integrations yield

$$\frac{-i}{\omega_0-\omega_k-\omega_M}\frac{1}{2\omega_0-\omega_E-\omega_M}\frac{1}{\omega_0-\omega_{k'}-\omega_E}.$$

The product of the color traces gives a factor of 2. The spatial integrals are

$$\int (\bar{q}_s \mathcal{A}^{\mathrm{TE}} q_k)(x)(\bar{q}_k \mathcal{A}^{\mathrm{TM}} q^C_{-s})(y) d^3x\, d^3y$$

$$= N_{0+}{}^2 N_{k+}{}^2 N_m^{\mathrm{TE}} N_m^{\mathrm{TM}} \frac{1}{2m(m+1)} \int \left[\chi_s^\dagger(\alpha j_0, i\alpha' \vec{\sigma}\cdot\hat{r} j_1) \begin{bmatrix} 0 & -\vec{\sigma} \\ \vec{\sigma} & 0 \end{bmatrix} \cdot \vec{\mathscr{L}} Y_{mn} j_m \begin{bmatrix} \alpha_k j_k \\ i\alpha'_k \vec{\sigma}\cdot\hat{r} j_{k+1} \end{bmatrix} \chi_{kl} \right](x)$$

$$\times \left[\chi^\dagger_{kl}(\alpha_k j_k, i\alpha'_k \vec{\sigma}\cdot\hat{r} j_{k+1}) \begin{bmatrix} 0 & -\vec{\sigma} \\ \vec{\sigma} & 0 \end{bmatrix} \cdot \vec{\mathcal{A}}^{\mathrm{TM}}_{m,-n} \begin{bmatrix} \alpha' \vec{\sigma}\cdot\hat{r} j_1 \\ i\alpha j_0 \end{bmatrix} \chi^C_{-s} \right](y) d^3x\, d^3y$$

$$\sim \int \chi_s^\dagger i \vec{\sigma}\cdot\hat{r} \times \vec{\mathscr{L}} Y_{mn} \chi_{kl} i(\alpha\alpha'_k j_0 j_{k+1} + \alpha' \alpha_k j_1 j_k) j_m d^3x$$

$$\times \int \chi^\dagger_{kl} \left[\frac{m(m+1)}{2m+1} i(j_{m-1} + j_{m+1}) \vec{\sigma}\cdot\hat{r} Y_{m,-n} i(\alpha'_k \alpha' j_{k+1} j_1 - \alpha_k \alpha j_k j_0) \right.$$

$$\left. + \frac{(m+1)j_{m-1} - m j_{m+1}}{2m+1} \vec{\sigma}\cdot\hat{r} \times \vec{\mathscr{L}} Y_{m,-n}(-i\alpha_k \alpha j_k j_0 - i\alpha'_k \alpha' j_{k+1} j_1) \right] \chi^C_{-s} d^3y \ . \tag{14}$$

These integrals are factorized into radial and angular parts. The products

$$\int \chi_s^\dagger \vec{\sigma}\cdot\hat{x} \times \vec{\mathscr{L}} Y_{mn} \chi_{kl} d\Omega_x \int \chi^\dagger_{kl} \vec{\sigma}\cdot\hat{y} \times \vec{\mathscr{L}} Y_{m,-n} \chi^C_{-s} d\Omega_y \tag{15}$$

and

$$\int \chi_s^\dagger \vec{\sigma}\cdot\hat{x} \times \vec{\mathscr{L}} Y_{mn} \chi_{kl} d\Omega_x \int \chi^\dagger_{kl} \vec{\sigma}\cdot\hat{y} Y_{m,-n} \tag{16}$$

are calculated simultaneously. Since the system has spherical symmetry, one integral can be evaluated at an arbitrary point, e.g., $\hat{x}$ can be chosen in the z direction. $Y_{kl}(\hat{z}) = \delta_{l0}[(2k+1)^{1/2} 4\pi]$ and $\int d\Omega_x$ is replaced by a factor of 4π. The only nonvanishing contributions come from

$$\int \chi_s^\dagger \vec{\sigma}\cdot\hat{x} \times \vec{\mathscr{L}} Y_{mn} \chi_{kl} d\Omega \to \mp i 4\pi \frac{1}{\sqrt{4\pi}} \sqrt{2} \left[\frac{m}{2}(m+1) \right]^{1/2} \left[\frac{2m+1}{4\pi} \right]^{1/2} \left[\frac{k+1}{2k+1} \right]^{1/2} \left[\frac{2k+1}{4\pi} \right]^{1/2}$$

$$= \begin{cases} -i \dfrac{1}{\sqrt{4\pi}} [m(m+1)]^{1/2} (2m+1)^{1/2} (k+1)^{1/2} & \text{for } s = \frac{1}{2},\ n = 1,\ l = -\frac{1}{2} \\ i \dfrac{1}{\sqrt{4\pi}} [m(m+1)]^{1/2} (2m+1)^{1/2} (k+1)^{1/2} & \text{for } s = -\frac{1}{2},\ n = -1,\ l = \frac{1}{2} \ . \end{cases} \tag{17}$$

It suffices to compute the other integral for $s = \frac{1}{2}$, $n = 1$, $l = -\frac{1}{2}$. The integral for $s = -\frac{1}{2}$ has the same value but the opposite sign. With the definitions

$$L^\pm = \frac{1}{\sqrt{2}}(L_x \pm i L_y), \quad \sigma^\pm = \frac{1}{\sqrt{2}}(\sigma_x \pm i\sigma_y), \quad r^\pm = \frac{1}{\sqrt{2}}(x \pm iy) = \mp \left[\frac{4\pi}{3} \right]^{1/2} Y_{1,\pm 1}, \quad r^0 = z = \left[\frac{4\pi}{3} \right]^{1/2} Y_{10} \ ,$$

$$\vec{\sigma}\cdot\vec{r} \times \vec{\mathscr{L}} = i(\sigma^- r^0 L^+ + \sigma^0 r^+ L^- + \sigma^+ r^- L^0 - \sigma^- r^+ L^0 - \sigma^0 r^- L^+ - \sigma^+ r^0 L^-) \ , \tag{18}$$

$$\int \chi^\dagger_{kl} \sigma\cdot\hat{y} \times \vec{\mathscr{L}} Y_{m,-n} \chi^C_{-s} d\Omega \to -i \int \chi^\dagger_{k,-1/2} \vec{\sigma}\cdot\hat{y} \times \vec{\mathscr{L}} Y_{m,-1} \chi_{1/2} d\Omega$$

$$= \int \frac{1}{(2k+1)^{1/2}} [\sqrt{k}\, Y^*_{k,-1} (k+1)^{1/2} Y_{k0}]$$

$$\times [\sigma_0(r^+ L^- - r^- L^+) + \sigma^-(r^0 L^+ - r^+ L^0)] Y_{m,-1} \begin{bmatrix} Y_{00} \\ 0 \end{bmatrix}$$

$$= \frac{1}{\sqrt{3}} \frac{1}{(2k+1)^{1/2}} \int (\sqrt{k}\, Y_{k1}(Y_{11} L^- Y_{m,-1} + Y_{1,-1} L^+ Y_{m,-1})$$

$$+ \sqrt{2}(k+1) Y_{k0} \{ [(m/2)(m+1)]^{1/2} Y_{10} Y_{m0} - Y_{11} Y_{m,-1} \}) d\Omega \ .$$

The use of the relations

$$\int Y_{k1}L^2Y_{10}Y_{m,-1}=k(k+1)\int Y_{k1}Y_{10}Y_{m,-1}$$
$$=2\int Y_{k1}(Y_{11}L^-Y_{m,-1}+Y_{1,-L}L^+Y_{m1})+[2+m(m+1)]\int Y_{k1}Y_{10}Y_{m,-1}\,,$$
$$\int Y_{k+1,1}Y_{k0}Y_{1,-1}=-\left[\frac{k+2}{2(k+1)}\right]^{1/2}\int Y_{k+1,0}Y_{k0}Y_{10},\quad \int Y_{k+1,1}Y_{k,-1}Y_{10}=-\frac{[k(k+2)]^{1/2}}{k+1}\int Y_{k+1,0}Y_{k0}Y_{10}\,, \tag{19}$$
$$\int Y_{k+1,0}Y_{k1}Y_{1,-1}=\left[\frac{k}{2(k+1)}\right]^{1/2}\int Y_{k+1,0}Y_{k0}Y_{10},\quad \int Y_{k+1,0}Y_{k0}Y_{10}=\left[\frac{3}{4\pi}\right]^{1/2}\frac{k+1}{[(2k+1)(2k+3)]^{1/2}}\,,$$

yields

$$=\frac{1}{\sqrt{4\pi}}\left[\frac{k+2}{2k+3}\right]^{1/2}(k+2)\delta_{m,k+1}\,. \tag{20}$$

Similarly

$$\int \chi^\dagger_{kl}\vec{\sigma}\cdot\hat{y}Y_{m,-n}\chi^C_{-s}d\Omega\to\frac{-i}{\sqrt{4\pi}}\left[\frac{k+2}{2k+3}\right]^{1/2}\delta_{m,k+1}\,. \tag{21}$$

Summing over s and interchanging quark and antiquark gives a factor of 2 each:

$$\to\int(\bar{q}_s\mathcal{A}^{\rm TE}q_k)(x)(\bar{q}_k\mathcal{A}^{\rm TM}q_s^C)(y)d^3x\,d^3y$$
$$=\frac{2}{4\pi}N_{0+}{}^2N_{k+}{}^2N_m^{\rm TE}N_m^{\rm TM}\int[\alpha\alpha'_kj_0(x_0r)j_{k+1}(x_kr)+\alpha'\alpha_kj_1(x_0r)j_k(x_kr)]j_m(x_Er)r^2dr$$
$$\times\left\{\int-\frac{m(m+1)}{2m+1}[j_{m-1}(x_MR)+j_{m+1}(x_MR)][\alpha'\alpha'_kj_1(x_0r)j_{k+1}(x_kr)\right.$$
$$-\alpha\alpha_kj_0(x_0r)j_k(x_kr)]r^2dr$$
$$+(m+1)\int\frac{(m+1)j_{m-1}(x_Mr)-mj_{m+1}(x_Mr)}{2m+1}[\alpha\alpha_kj_0(x_0r)j_k(x_kr)$$
$$\left.+\alpha'\alpha'_kj_1(x_0r)j_{k+1}(x_kr)]r^2dr\right\}, \tag{22}$$

where $k=m-1$. This result was multiplied by the two other integrals, which gave a similar factor, and divided by $2r+1$ to symmetrize the intermediate state. The result is

$$\tfrac{4}{3}\alpha_s{}^2\frac{1}{2r+1}(N_m^{\rm TE}N_m^{\rm TM})^2N_{0+}{}^4N_{(m-1)+1/2}{}^2N_{m+1/2}{}^2\frac{1}{\omega_0-\omega_m-\omega_E}\frac{1}{\omega_0-\omega_{m-1}-\omega_M}\frac{1}{2\omega_0-\omega_E-\omega_M}\frac{1}{R}$$
$$\times\int\left[\alpha\alpha_{m-1}j_0(x_0r)j_{m-1}(x_{m-1}r)(m+1)j_{m-1}(x_Mr)\right.$$
$$\left.+\alpha'\alpha'_{m-1}j_1(x_0r)j_m(x_{m-1}r)\frac{(m+1)j_{m-1}(x_Mr)-2m(m+1)j_{m+1}(x_Mr)}{2m+1}\right]r^2dr$$
$$\times\int\left[\alpha\alpha'_mj_0(x_0r)j_{m+1}(x_mr)mj_{m+1}(x_Mr)-\alpha'\alpha_mj_1(x_0r)j_m(x_mr)\frac{2m(m+1)j_{m-1}(x_Mr)+mj_{m+1}(x_Mr)}{2m+1}\right]r^2dr$$
$$\times\int[\alpha\alpha'_{m-1}j_0(x_0r)j_m(x_{m-1}r)+\alpha'\alpha_{m-1}j_1(x_0r)j_{m-1}(x_{m-1}r)]j_m(x_Er)r^2dr$$
$$\times\int[\alpha\alpha_mj_0(x_0r)j_m(x_mr)+\alpha'\alpha'_mj_1(x_0r)j_{m+1}(x_mr)]j_m(x_Er)r^2dr\,. \tag{23}$$

The results of the calculation can be summarized as follows: For a given angular momentum of the intermediate gluons the time ordering of the interaction vertices determines uniquely the value of the angular momentum for the intermediate quark, once the choice for $j=l+\frac{1}{2}$ or $j=l-\frac{1}{2}$ quarks is made.

Other diagrams are calculated in a similar way. Owing to the complexity of the procedures we will not repeat the above presentation for each diagram but just give numerical results in the next section.

IV. RESULTS

In Table I several of the intermediate results are displayed. The light-quark mass was taken as $m_u=m_d=0$, and these results, in units of α_s^2/R, are independent of R. The strange-quark mass was $m_s=300$ MeV, and in this case we used $m_sR=1$. One can see from these results that diagrams with two physical gluons do give a negative-energy shift, as expected. However, those diagrams which involve the Coulomb interaction are positive and much larger. As might be expected, the largest single diagram is that which has the smallest energy denominators, involving $1S_{1/2}$ quarks and the lowest TE gluon mode. Diagrams involving first radial excited states contribute typically less than 1% of the ground-state value in the Coulomb case and about 5% in the two-gluon fusion process. It is the dominance of the Coulomb interaction which allows the mass shift to be positive.

Summing all contributions the results are

$$\begin{aligned}\langle \bar{u}u \mid H_{\text{eff}} \mid \bar{u}u \rangle &= 0.39\alpha_s^2/R \ , \\ \langle \bar{u}u \mid H_{\text{eff}} \mid \bar{s}s \rangle &= 0.29\alpha_s^2/R \ , \\ \langle \bar{s}s \mid H_{\text{eff}} \mid \bar{s}s \rangle &= 0.18\alpha_s^2/R \ .\end{aligned} \tag{24}$$

These numbers are relatively large and are capable of shifting the η' mass to its observed position. Note also that SU(3) breaking is considerable. It turns out that because of the approximately linear dependence on the number of strange quarks, the effect of the SU(3) breaking on the η,η' masses is not as large as one would think. In order to assess the effect of these results, we have used them to calculate the η and η' masses. Following the procedure of Donoghue and Johnson,[3] the bag energy is identified with the energy of the wave packet which describes the bag state

$$\langle (p^2+m^2)^{1/2} \rangle = E_{\text{bag}} \ . \tag{25}$$

In this manner an octet of massless pseudoscalars can be found when the quark masses are zero, if the bag-model parameters are suitably adjusted. The pion and kaon masses can then be understood by turning on the quark masses to shift these states to their physical values. This has been performed at order α_s, with the resulting value $\alpha_s \simeq 2$. Other estimates of α_s in the bag model[2] produce a range $\alpha_s=1\rightarrow 2.2$. Use of the $\alpha_s=2$ would put the η' mass too high. However, this value of α_s would be modified if the calculation of the pion and kaon masses were carried out to $O(\alpha_s^2)$. Our procedure will be to set the pion and kaon masses at their physical values, and from these calculate what the base $(u\bar{u}+d\bar{d})$ and $s\bar{s}$ masses are without the annihilation diagram. The annihilation diagram will then be added, the bag energy diagonalized, and α_s adjusted in order to reproduce the particle masses as closely as possible. This procedure will be counted as successful if we can reproduce the masses using a value of α_s reasonably close to the lowest-order value. In the basis $(1/\sqrt{2})(u\bar{u}+d\bar{d})$ and $s\bar{s}$, the isoscalar bag energy matrix is

$$E=\begin{bmatrix} E_\pi & 0 \\ 0 & 2E_K-E_\pi \end{bmatrix} + \frac{\alpha_s^2}{R}\begin{bmatrix} 0.78 & 0.41 \\ 0.41 & 0.18 \end{bmatrix} , \tag{26}$$

where

$$\begin{aligned} E_\pi &= \langle (p^2+m_\pi^2)^{1/2} \rangle = 0.616 \text{ GeV} \ , \\ E_K &= \langle (p^2+m_K^2)^{1/2} \rangle = 0.778 \text{ GeV} \ , \end{aligned} \tag{27}$$

and the second term is the effect of the annihilation diagram. We will use a common value of R in the diagonalization, as the overlaps are well defined only in this case. However, the physical states most likely have different values of R. This would lead to some changes in the detailed results, but the overall feature should be unchanged.

With a value $\alpha_s=1.15$, the masses are

$$m_\eta = 530 \text{ MeV}, \quad m_{\eta'} = 965 \text{ MeV} \tag{28}$$

and the mixing angle is $\theta=37°$. As this was a one-parameter fit, we feel that the agreement on the masses is excellent, and that the value of α_s is reasonable. As a check on the consistency of this result we have looked at the vector mesons to see if the same type of diagram would produce too large a ω-ϕ mixing. The annihilation

TABLE I. Second-order energy corrections in units of α_s^2/R for pseudoscalars due to quark-gluon fusion for $m_u=0$, $m_s=300$ MeV, $R=3.3$ GeV^{-1}.

	Coulomb interaction			Two-gluon-fusion diagrams		
L_{Gluon}	$\bar{u}u\ \bar{u}u$	$\bar{u}u\ \bar{s}s$	$\bar{s}s\ \bar{s}s$	$\bar{u}u\ \bar{u}u$	$\bar{u}u\ \bar{s}s$	$\bar{s}s\ \bar{s}s$
1	0.306 10	0.250 07	0.182 48	−0.018 26	−0.030 69	−0.050 55
2	0.059 96	0.049 38	0.038 73	−0.003 39	−0.005 11	−0.007 20
3	0.019 77	0.016 08	0.012 75	−0.001 01	−0.001 46	−0.001 42
4	0.008 44	0.006 77	0.005 34	−0.000 38	−0.000 54	−0.000 68
5	0.004 22	0.003 33	0.002 61	−0.000 17	−0.000 24	−0.000 29

diagram in the vector mesons must proceed through three gluons. We have not performed a complete calculation but have only included those diagrams which are similar to the dominant ones from the pseudoscalar case. We estimate that the energy corrections are 4—8 % of those in $\eta\eta'$ systems and that the mass shifts involved are less than 30 MeV (the direction improves the agreement with the physical values).

V. SUMMARY

We have calculated the contributions of the annihilation diagrams to the $\eta\eta'$ masses at $O(\alpha_s{}^2)$. The resulting energy shift is large and positive. The Coulomb interaction plays an important role in making this number positive. In particular, it is *not* appropriate to consider the Feynman diagram of Fig. 1 as mixing with a glueball, as is done in many phenomenological analyses.[10] Since the dominant contribution does not contain two physical gluons, and since mixing generates the incorrect sign, such approaches would not be expected to be reasonable.

The spectroscopy which results from this calculation is very encouraging. The pion and kaon masses can always be fit by adjustment of the quark masses. With a reasonable value of $\alpha_s=1.15$, we then would find $m_\eta=530$ MeV, $m_{\eta'}=965$ MeV. The precise values of our results may have considerable uncertainty as they come from a one-loop process, the study of which is rather new in the bag model. In addition, this is the first bag-model calculation which has been done to $O(\alpha_s{}^2)$. However, even substantial changes in our results could be accommodated phenomenologically without modifying the quality of the spectrum by readjustment of α_s. What is clear is that the annihilation-diagram mechanism for generating the mass of the η' in quark models does appear to work, and that the $J^{PC}=0^{-+}$ masses in the bag model can easily reproduce the observed spectrum.

ACKNOWLEDGMENTS

We would like to thank H. Hansson, R. Jaffe, K. Johnson, and N. Isgur for useful comments on this subject. This work was supported in part by the National Science Foundation.

[1]A. Chodos, R. L. Jaffe, K. Johnson, C. B. Thorn, and V. F. Weisskopf, Phys. Rev. D 9, 3471 (1974); T. DeGrand, R. L. Jaffe, K. Johnson, and J. Kiskis, *ibid.* 12, 2060 (1975).

[2]More references to bag phenomenology can be found in C. DeTar and J. F. Donoghue, in Ann. Rev. Nucl. Part. Sci. 33, (1983).

[3]J. F. Donoghue and K. Johnson, Phys. Rev. D 21, 1975 (1980).

[4]S. Weinberg, Phys. Rev. D 11, 3583 (1975).

[5]S. Adler, Phys. Rev. 177, 2426 (1969); J. Bell and R. Jackiw, Nuovo Cimento 60A, 47 (1969).

[6]E. Witten, Nucl. Phys. B156, 269 (1979).

[7]A. De Rújula, H. Georgi, and S. L. Glashow, Phys. Rev. D 12, 147 (1975).

[8]A. Maciel and S. Monaghan, Oxford Report No. Oxford 25/82, 1982 (unpublished).

[9]R. Friedberg and T. D. Lee, Phys. Rev. D 18, 2623 (1978).

[10]P. M. Fishbane, G. Karl, and S. Meshkov, Report No. UCLA/82/TEP/18 (unpublished); T. Teshima and S. Oneda, Phys. Rev. D 27, 1551 (1983); W. Palmer and S. Pinsky, *ibid.* 27, 2219 (1983).